Eur. Phys. J. Appl. Phys. **29**, 209–213 (2005)
DOI: 10.1051/epjap:2004219

THE EUROPEAN PHYSICAL JOURNAL APPLIED PHYSICS

Influence of high-index GaAs substrates on the 2D electron density of δ-doped pHEMT with an additional $In_xGa_{1-x}As$ ($x > 0.15$) thin layer embedded in the channel

L. Bouzaïene[a], S. Rekaya, L. Sfaxi, and H. Maaref

Laboratoire de Physique des Semiconducteurs et des Composants Électroniques, Faculté des Sciences de Monastir, avenue de l'Environnement, 5000 Monastir, Tunisia

Received: 10 May 2004 / Accepted: 7 October 2004
Published online: 21 December 2004 –

Abstract. In this paper, we report the theoretical predictions of a high-index GaAs substrate ((111)A and (311)A) on the subband structure and thereafter on the 2D electron density of Si δ-doped $Al_{0.33}Ga_{0.67}As/In_{0.15}Ga_{0.85}As/GaAs$ pseudomorphic high electron mobility transistor (pHEMT) with an additional $In_xGa_{1-x}As$ ($x > 0.15$) thin layer embedded in the channel. We have seen that the electronic structures and the electron density are quite sensitive to the additional $In_xGa_{1-x}As$ ($x > 0.15$) layer thickness, indium composition and to their position in the channel. An optimal position of the additional $In_xGa_{1-x}As$ layer was found to be corresponding to the maximum of the first eigen envelope function for the different growth directions. We report that the optimised electron density is obtained in the structure grown on (111)A GaAs substrate. In this case the electron transfer is significantly higher than those grown on (311)A and (001) GaAs substrates respectively.

PACS. 73.20.At Surface states, band structure, electron density of states –
73.40.Kp III-V semiconductor-to-semiconductor contacts, p-n junctions, and heterojunctions

1 Introduction

The pseudomorphically strained InGaAs layer has been demonstrated to be an excellent channel layer for the modulation-doped AlGaAs/InGaAs/GaAs pseudomorphic high electron mobility transistors (pHEMTs). Such a pHEMT structure has led to considerable improvement in device performance [1–4] due to the increased conduction band discontinuity, which allows high electron densities to be achieved, even when low Al content barriers are used to minimize the presence of DX centers. Such a structure grown on substrates with orientation different from (001) has been gaining attention because of the presence of a built-in electric field, generated via piezoelectric effects, the ability to grow (III−V) heterostructures on (N11) substrates provides a further degree of freedom for electro-optical devices [5,6]. Electrons are confined at the heterojunction not only by their electrostatic attraction to ionized impurities in the large gap AlGaAs layer, but also by the presence of an InGaAs quantum well. Increasing the In composition facilitates higher performance in these pHEMTs. However, it has been difficult to increase the In composition past 0.3 because In segregation limits the critical layer thickness, making it thinner than the calculated one [7]. To overcome such problem, in this work we added an $In_xGa_{1-x}As$ ($x > 0.15$) thin layer embedded in the channel of $Al_{0.33}Ga_{0.67}As/In_{0.15}Ga_{0.85}As/GaAs$ pHEMT. The aim of this work is to predict the charge transfer in this type of structure for three different growth directions, such as (001), (111) and (311). A few structures have been grown previously on (111)B oriented substrates because they provide the largest built-in electric field. The (111)A oriented substrates provide the same built-in electric field but crystal growth is by far more difficult [8]. The electric field in strained quantum wells (SQWs) grown on gallium terminated (A) substrates has the opposite direction of the electric field in SQWs grown on arsenic terminated (B) substrates [9]. Similar behavior has been reported on (311)A/B oriented substrates [6]. The above properties have been used in this work to predict more charge transfer in pHEMT devices. We have chosen the (111)A and (311)A GaAs substrates because the charge transfer in pHEMT structures is reduced when the layers are grown on GaAs (111)B substrates as previously reported [10]. We have studied theoretically the influence of an additional $In_xGa_{1-x}As$ ($x > 0.15$) layer in the $In_{0.15}Ga_{0.85}As$ channel layer on the electron density by solving the Schrödinger and Poisson equations

[a] e-mail: boulotf@yahoo.fr

self-consistently. The numerical procedure adopted in this work is the finite differential. In addition, the total potential includes a local exchange-correlation potential term, and we have taken into account the strain effects in our calculations.

2 Theoretical considerations

The structure under investigation consists of epitaxial layers grown from the bottom to the top as: an undoped GaAs buffer layer, a 10 nm undoped $In_{0.15}Ga_{0.85}As$ channel, a 10 nm undoped $Al_{0.33}Ga_{0.67}As$ spacer layer, a 2×10^{12} cm^{-2} Si δ-doping layer, an undoped $Al_{0.33}Ga_{0.67}As$ barrier, and an undoped GaAs cap layer for three different GaAs substrate orientations, such as (001), (111)A and (311)A. An additional $In_xGa_{1-x}As$ ($x > 0.15$) thin layer was added to the structure (embedded in the channel). The electronic structure of the Si δ-doped AlGaAs/InGaAs/GaAs heterostructure has been investigated by using a self-consistent calculation in the effective mass approximation. The problem to be solved is reduced to a series of one-body equations. We have considered, on the other hand, the system at low temperature and no external electric field is applied on the structure under investigation. We have calculated the confining potential, the electron density, the subband energies, the eigen envelope wave functions and the Fermi energy level self-consistently by solving simultaneously the Schrödinger and Poisson equations.

The Schrödinger equation is:

$$\left[-\frac{\hbar^2}{2}\frac{1}{m^*(z)}\frac{d^2}{dz^2} + V(z)\right]\Psi_i(z) = E_i\,\Psi_i(z).$$

Here, z is the growth direction, $m^\star(z)$ being the electron effective mass at the bottom of the Γ conduction band. E_i and Ψ_i are the quantized energy levels and their corresponding electronic wave function, respectively. The potential $V(z)$ is the total energy split for different contributions into:

$$V(z) = V_b(z) + V_H(z) + V_{XC}(z) + V_{pz}(z)$$

where $V_b(z)$ is the conduction band edge potential without doping, $V_{XC}(z)$ the exchange-correlation potential which is induced by the many-body effects and whose expression is taken from [11]:

$$V_{XC}(z) = -\,0.916\frac{e^2}{6\pi\varepsilon_0\,\varepsilon_r}\left[\frac{3n(z)}{4\pi}\right]^{1/3}$$

$V_{pz}(z)$ is the piezoelectric potential and can be written as:

$$V_{pz}(z) = eFz$$

where F is the magnitude of the piezoelectric field in the strained InGaAs layer, $V_H(z)$ is the effective Hartree potential, obtained by solving the Poisson equation:

$$\frac{d}{dz}\left[\varepsilon_r(z)\frac{d}{dz}V_H(z)\right] = \frac{e^2}{\varepsilon_0}\left[N_d(z) - N_a(z) - n(z)\right].$$

Here, $\varepsilon_r(z)$ is the relative local dielectric constant of the different layers, $N_a(z)$ is the residual acceptor concentration, $N_d(z)$ is the total density of ionised dopants (we have taken a Dirac distribution form) and $n(z)$ is the local density of confined electrons. The latter is related to wave functions $\Psi_i(z)$ by the following relation:

$$n(z) = \sum_i n_i\,|\Psi_i(z)|^2.$$

At low temperature n_i can be written as:

$$n_i = \frac{m^*}{\pi\hbar^2}\,(E_F - E_i)$$

where n_i is the carrier population in the ith subband and E_F is the Fermi level. At low temperature, E_F is pinned at the DX center energy [12]. For more details of theoretical considerations, see our previous work [13]. In evaluating the total potential energy, we have taken into account the strain effects [13].

We have adopted the same theoretical method (finite differential method) in our previous work [14]. In addition, it is important to indicate that in our previous works [14,15] we have tested the validity of our calculation for different types of heterostructures such as the conventional and pseudomorphic ones and we have obtained a good agreement with the experimental results.

3 Results and discussion

As a system, we consider an n-type δ-doped $Al_{0.33}Ga_{0.67}As/In_{0.15}Ga_{0.85}As/GaAs$ with and without an additional $In_xGa_{1-x}As$ ($x > 0.15$) thin layer embedded in the channel. We have calculated for these heterostructures the conduction band edge, the energy levels and wave functions of the confined electronic states for three different growth directions, such as (001), (111)A and (311)A. Figures 1a–c show the conduction band structure for δ-doped AlGaAs/InGaAs/GaAs without the additional $In_xGa_{1-x}As$ ($x > 0.15$) layer for (001), (111)A and (311)A growth directions respectively. For (001) growth direction there is no piezoelectric field. The potential is deeper to the left, near the doped AlGaAs barrier and the first wave function is displaced towards the left. The situation is completely different for the (111)A growth direction where the piezoelectric field gives a potential, which is much deeper to the right, near the GaAs undoped barrier. The electrons are now concentrated to the right half of the InGaAs channel layer. While for (311)A growth direction, we note a weak piezoelectric field. The total potential is slightly deeper to the left, near the AlGaAs barrier and the electrons are concentrated in the middle of the InGaAs quantum well. In Table 1, we show the electron density obtained in $Al_{0.33}Ga_{0.67}As/In_{0.15}Ga_{0.85}As/GaAs$ heterostructure (without an additional $In_xGa_{1-x}As$ thin layer) and the positions of the first envelope wavefunctions maximum relatives to the left interface for the (001), (111)A and

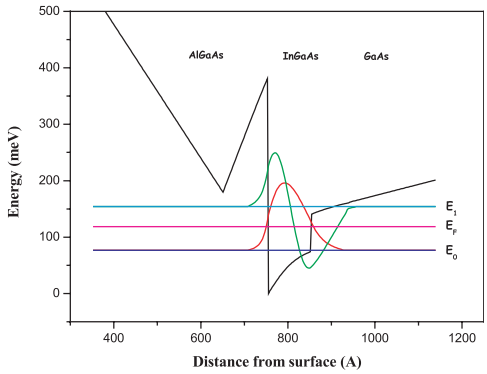

(a)

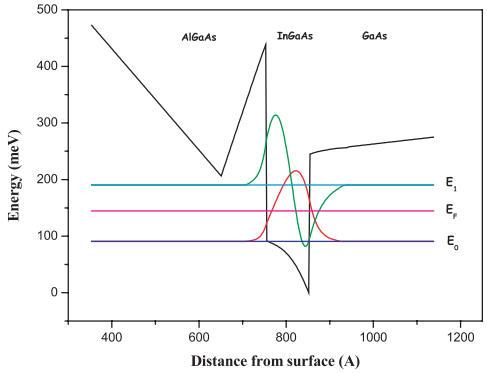

(b)

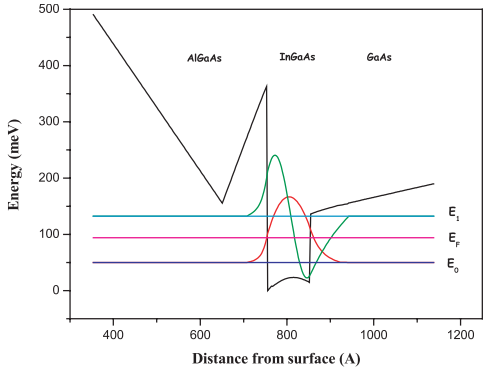

(c)

Fig. 1. (a) The self-consistent calculation of the conduction band structure, the levels energy, and the corresponding wavefunctions for δ-doped $Al_{0.33}Ga_{0.67}As/In_{0.15}Ga_{0.85}As/GaAs$ pseudomorphic structure grown on (001) GaAs oriented substrate. With donor concentration $N_d^{2D} = 2 \times 10^{12}$ cm^{-2}, channel thickness = 10 nm, and spacer = 10 nm at low temperature. (b) The self-consistent calculation of the conduction band structure, the levels energy, and the corresponding wavefunctions for δ-doped $Al_{0.33}Ga_{0.67}As/In_{0.15}Ga_{0.85}As/GaAs$ pseudomorphic structure grown on (111)A GaAs oriented substrate. With donor concentration $N_d^{2D} = 2 \times 10^{12}$ cm^{-2}, channel thickness = 10 nm, and spacer = 10 nm at low temperature. (c) The self-consistent calculation of the conduction band structure, the levels energy, and the corresponding wavefunctions for δ-doped $Al_{0.33}Ga_{0.67}As/In_{0.15}Ga_{0.85}As/GaAs$ pseudomorphic structure grown on (311)A GaAs oriented substrate. With donor concentration $N_d^{2D} = 2 \times 10^{12}$ cm^{-2}, channel thickness = 10 nm, and spacer = 10 nm at low temperature.

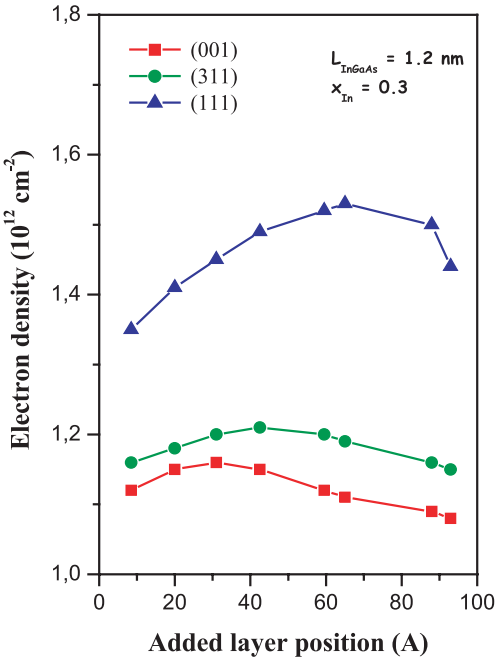

Fig. 2. Variation of the electron density at low temperature as a function of the position of the additional $In_{0.3}Ga_{0.7}As$ thin layer embedded in the channel in relation to the left interface with $L_{InGaAs} = 1.2$ nm.

Table 1. Electron density in δ-doped $Al_{0.33}Ga_{0.67}As/In_{0.15}Ga_{0.85}As/GaAs$ pseudomorphic structure without an additional InGaAs thin layer and the positions of the first envelope wavefunctions maximum per head of the left interface for (001), (111)A, and (311)A growth directions, with channel thickness = 10 nm.

GaAs substrate orientation	(001)	(311)A	(111)A
Electron density (10^{12} cm^{-2})	1.06	1.13	1.39
Position of the first wavefunction maximum (nm)	3.3	4.5	6.7

(311)A growth directions, with a channel thickness equal to 10 nm. Then, increasing the indium composition in the channel facilitates higher performance in these pHEMTs. However, increase the In composition has been greatly difficult, especially when the channel thickness is large, because In segregation limits the critical layer thickness [16,17]. To overcome such problem, we use an additional $In_xGa_{1-x}As$ ($x > 0.15$) thin layer embedded in the channel of $Al_{0.33}Ga_{0.67}As/In_{0.15}Ga_{0.85}As/GaAs$ pHEMT. Figure 2 shows the results of the calculation of the electron density, at low temperature, as a function of the additional $In_{0.3}Ga_{0.7}As$ layer position in the channel in relation to the AlGaAs/InGaAs interface for three different growth directions. The thickness of the embedded $In_{0.3}Ga_{0.7}As$ layer was fixed at 1.2 nm. We have observed that the optimal positions of the additional $In_{0.3}Ga_{0.7}As$

layer for maximum electron density are found to be 3.1 nm, 4.3 nm and 6.5 nm for (001), (311)A, and (111)A growth directions respectively. These values correspond exactly to the position of the first eigen envelope function maximum for the different growth directions. In this context, we report in Figures 3a–c the conduction band structure for the δ-doped AlGaAs/InGaAs/GaAs with the additional $In_{0.3}Ga_{0.7}As$ layer (1.2 nm) embedded at the position of the first eigen envelope function maximum for the (001), (111)A and (311)A growth directions respectively. We note that the electron subbands and their corresponding wave functions are sensitive to the additional $In_{0.3}Ga_{0.7}As$ layer in the channel. However, in our investigation of the electron density there are two important parameters: the indium concentration and the thickness of the added $In_xGa_{1-x}As$ ($x > 0.15$) layer. Figure 4 shows the results of the calculation of the electron density, at low temperature, as a function of indium concentration for three different growth directions. The thickness of the embedded InGaAs layer was fixed at 1.2 nm. We have observed that the calculated electron density in the structure grown on (111)A GaAs substrate is significantly higher than those grown on (311)A and (001) GaAs substrates respectively. Moreover, this enhancement is for several different indium concentrations. Later, we explain this electron density evolution by the increased conduction band discontinuity and consequently a good electron confinement has been achieved. In addition, this improvement is due to the incorporation of a piezoelectric field within the pseudomorphically strained active layer in the structures grown on (111)A and (311)A GaAs substrates. We also note a significant increase of 24% in the electron density (between with and without the additional $In_xGa_{1-x}As$ layer embedded in the channel), when the growth direction is (111)A and the indium concentration is equal to 0.5. A similar behaviour is seen in Figure 5, in which the additional InGaAs layer thickness is varied for a fixed indium mole fraction of 0.3 and their position is at the position of the first wave function maximum. The enhancement of the electron density was explained by the widening of the channel layer formed by the InGaAs. Therefore, the difference between subband energies and Fermi level increases. It can be seen that, the piezoelectric effects are the largest for the larger embedded InGaAs layer thickness. We note a significant increase of 38% in the electron density (between with and without the additional $In_{0.3}Ga_{0.7}As$ layer embedded in the channel), when the added layer thickness is equal to 4.5 nm. We have limited our comparison only to (111)A direction, as the electron density in (111)A direction is higher than in (311)A and (001) directions for different indium concentration and additional InGaAs layer thickness.

4 Conclusion

In conclusion, we have calculated the electronic subband structure of Si δ-doped AlGaAs/InGaAs/GaAs pHEMT for three different growth directions, (001), (111)A, and

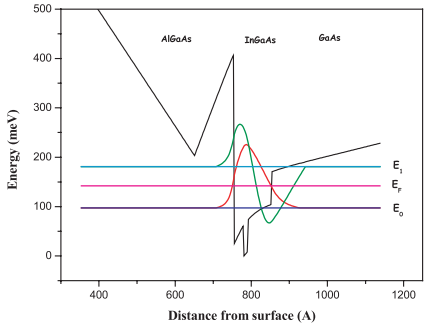

(a)

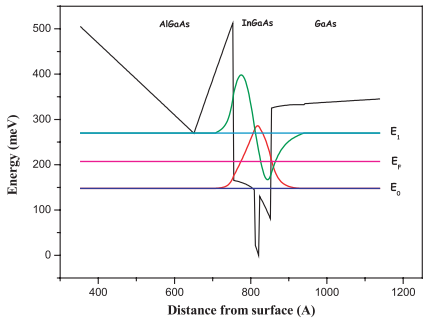

(b)

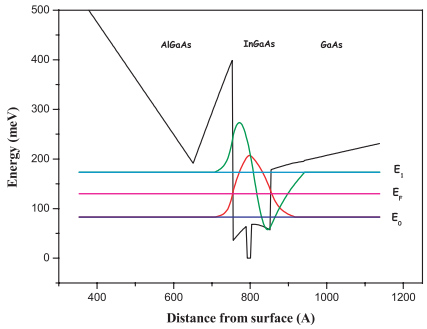

(c)

Fig. 3. (a) The self-consistent calculation of the conduction band structure, the levels energy, and the corresponding wavefunctions for δ-doped $Al_{0.33}Ga_{0.67}As/In_{0.15}Ga_{0.85}As/GaAs$ pseudomorphic structure, with an additional $In_{0.3}Ga_{0.7}As$ thin layer (1.2 nm) embedded in the channel, grown on (001) GaAs oriented substrate. With donor concentration $N_d^{2D} = 2 \times 10^{12}$ cm^{-2}, channel thickness = 10 nm, and spacer = 10 nm at low temperature. (b) The self-consistent calculation of the conduction band structure, the levels energy, and the corresponding wavefunctions for δ-doped $Al_{0.33}Ga_{0.67}As/In_{0.15}Ga_{0.85}As/GaAs$ pseudomorphic structure, with an additional $In_{0.3}Ga_{0.7}As$ thin layer (1.2 nm) embedded in the channel, grown on (111)A GaAs oriented substrate. With donor concentration $N_d^{2D} = 2 \times 10^{12}$ cm^{-2}, channel thickness = 10 nm, and spacer = 10 nm at low temperature. (c) The self-consistent calculation of the conduction band structure, the levels energy, and the corresponding wavefunctions for δ-doped $Al_{0.33}Ga_{0.67}As/In_{0.15}Ga_{0.85}As/GaAs$ pseudomorphic structure, with an additional $In_{0.3}Ga_{0.7}As$ thin layer (1.2 nm) embedded in the channel, grown on (311)A GaAs oriented substrate. With donor concentration $N_d^{2D} = 2 \times 10^{12}$ cm^{-2}, channel thickness = 10 nm, and spacer = 10 nm at low temperature.

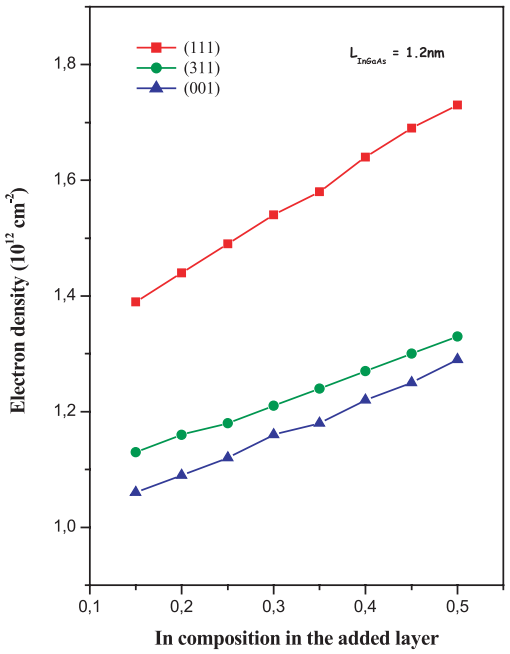

Fig. 4. Electron density at low temperature as a function of the indium concentration in the additional InGaAs thin layer (1.2 nm) embedded in the channel.

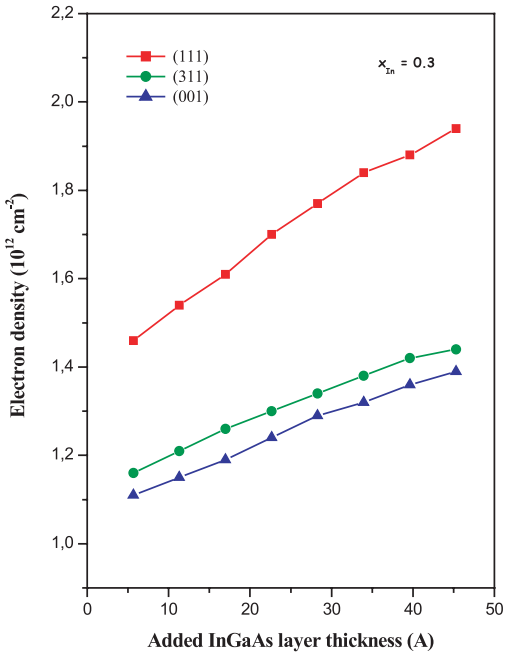

Fig. 5. Influence of the added InGaAs layer thickness on the electron density, at low temperature, with $x_{\mathrm{In}} = 0.3$.

(311)A containing an additional $In_xGa_{1-x}As$ ($x > 0.15$) thin layer embedded in the channel. The effects of the varied InGaAs thickness, In composition and position in relation to the left channel interface of the added layer on the electron density were studied theoretically. It was found that the embedded InGaAs layer could increase the electron density. It is worth noting that, to have a large electron density we must use a (111)A substrate and introduce the additional $In_xGa_{1-x}As$ ($x > 0.15$) layer exactly at the position of the first wave function maximum in the $In_{0.15}Ga_{0.85}As$ channel. Also, with the optimal structure, we have obtained an improvement of the electron density compared to that of the structure without any additional layer.

References

1. S.W. Chen, P.M. Smith, S.J. Liu, W.F. Kopp, T.J. Rogers, IEEE Microw. Guided W. **5**, 201 (1995)
2. J.J. Brown et al., IEEE Microw. Guided W. **6**, 91 (1996)
3. R. Grundbacher, A.A. Kettersonm, Y.C. Kao, I. Adesida, IEEE T. Electron Dev. **44**, 2136 (1997)
4. M.H. Somerville, J.A. Del Alamom, P. Saunier, IEEE T. Electron Dev. **45**, 1883 (1998)
5. P. Boring, B. Gil, K. Moore, Phys. Rev. Lett. **71**, 1875 (1993)
6. P.O. Vaccaro, M. Takahashi, K. Fujita, T. Watanabe, Jpn J. Appl. Phys. **34**, Part 2, L13 (1995)
7. H. Toyoshima, T. Niwa, J. Yamazaki, A. Okamoto, Appl. Phys. Lett. **63**, 821 (1993)
8. O. Brandt et al., Phys. Rev. B **48**, 17599 (1993)
9. P.O. Vaccaro, K. Tominaga, M. Hosoda, K. Fujita, T. Watanabe, Jpn J. Appl. Phys. **34**, Part 1, 1362 (1995)
10. L. Konczewicz, B. Jouault, S. Contreras, M.L. Sadowski, J.L. Robert, S. Blanc, Ch. Fontaine, Phys. Stat. Sol. B **223**, 507 (2001)
11. P. Ruden, G.H. Dohler, Phys. Rev. B **27**, 3538 (1983)
12. A. Leuther, A. Föster, H. Lüth, H. Holzbercher, U. Breur, Semicond. Sci. Technol. **11**, 766 (1996)
13. L. Bouzaïene, S. Rekaya, H. Sghaeïr, L. Sfaxi, H. Maaref, Appl. Phys. A **80**, 295 (2005)
14. L. Bouzaïene, L. Sfaxi, H. Sghaeïr, H. Maaref, J. Appl. Phys. **85**, 8223 (1999)
15. L. Bouzaïene, L. Sfaxi, H. Maaref, Microelectron. J. **30**, 705 (1999)
16. J.W. Matthews, A.E. Blakeslee, J. Cryst. Growth **27**, 118 (1974)
17. A. Polimeni, A. Patane, M. Henini, L. Eaves, P.C. Main, S. Sanguinetti, M. Guzzi, J. Cryst. Growth **201/202**, 276 (1999)